Contribution from the Departments of Chemistry, Ben Gurion University of the Negev, Beer-Sheva, Israel, and University of Rhode Island, Kingston, Rhode Island 02881, and from the Nuclear Research Centre Negev, Beer-Sheva, Israel

Stabilization of the Tervalent Nickel Complex with *meso*-5,7,7,12,14,14-Hexamethyl-1,4,8,11-tetraazacyclotetradecane by Axial Coordination of Anions in Aqueous Solution

ESTHER ZEIGERSON,[1a] ILANA BAR,[1a] JOEL BERNSTEIN,*[1a] LOUIS J. KIRSCHENBAUM,*[1a,b] and DAN MEYERSTEIN*[1a,c]

Received December 12, 1980

The electrochemical oxidation of NiL^{2+} (where L = *meso*-5,7,7,12,14,14-hexamethyl-1,4,8,11-tetraazacyclotetradecane) in aqueous solutions in the presence of sulfate, phosphate, chloride, and phthalate yields $Ni^{III}LX_2$. The stability constants for the axial coordination of the anions X are estimated from the observed redox potentials and from kinetic measurements. The complexes $[Ni^{III}L(SO_4)H_2O]ClO_4$ and $[Ni^{III}L(H_2PO_4)_2]ClO_4$ were precipitated. The crystal structure of the latter complex was determined. The complex crystallizes in the triclinic space group $P\bar{1}$ with a = 11.074 (3) Å, b = 9.386 (2) Å, c = 14.299 (2) Å, α = 88.55 (1)°, β = 106.33 (2)°, γ = 111.46 (2)°, and two molecules in the unit cell; least-squares refinement based on 4282 reflections led to a conventional R of 0.046. The nickel is located in the plane determined by the four ligating nitrogen atoms, and the configuration of the remainder of the macrocyclic ligand is essentially identical with that reported for the divalent nickel complex with this ligand. The kinetics of decomposition of the complexes were studied and found to be complicated. The results indicate that the complexes $Ni^{III}L(SO_4)_2^-$ and $Ni^{III}L(H_2PO_4^-)_2^+$ decompose via $Ni^{III}L^{3+}$ and perhaps also partially via $Ni^{III}LSO_4^+$ and $Ni^{III}LH_2PO_4^{2+}$. On the other hand decomposition of the complex $Ni^{III}LCl_2^+$ is predominantly via $Ni^{III}LCl^{2+}$ with partial decomposition via $Ni^{III}LCl_2^+$.

Introduction

Complexes of tervalent nickel with tetraaza macrocyclic ligands are readily prepared by electrochemical oxidation in aprotic media.[2,3] Tervalent nickel complexes with amines,[4] amino acids,[4,5] peptides,[6] and tetraaza macrocycles[7-9] have also been reported as relatively short-lived transients in aqueous solutions.

Recently we have shown using pulse radiolytic techniques that sulfate stabilizes the tervalent nickel complex with *meso*-5,7,7,12,14,14-hexamethyl-1,4,8,11-tetraazacyclotetradecane.[10] However the results of this study did not provide a full picture of the factors leading to the stabilization. The pulse radiolytic results indicated that the equilibrium reaction

$$NiL^{3+} + SO_4^{2-} \rightleftharpoons NiLSO_4^+ \qquad K_1 = 3 \times 10^3\ M^{-1} \text{ at } \mu = 0.3 \tag{1}$$

occurs[10] and that the product $NiLSO_4^+$ has an absorption spectrum[10] similar to that of the product obtained electrochemically.[11] However, the half-life of $NiLSO_4^+$ in 0.1 M SO_4^{2-} is ca. 5×10^5 times longer than that of NiL^{3+},[11] an observation that cannot be accounted for by the equilibrium reaction (1) even if $NiLSO_4^+$ decomposes only via NiL^{3+}. Furthermore, preliminary electrochemical measurements[11] indicated that $E°(NiL^{3+}/NiL^{2+}) \geq 1.2$ V vs. NHE, i.e., $E°$ is over 0.1 V higher than that predicted from K_1.

We therefore decided to extend our studies on the factors leading to the stabilization of NiL^{3+} by sulfate and to extend them to other ions, i.e., phosphate, chloride, and phthalate. The results indicated that the major form of $Ni^{III}L$ in solutions containing high concentration of ligating anions, X, is $Ni^{III}LX_2$.

Experimental Section

Materials. The complex $NiL(ClO_4)_2$ was synthesized according to published procedures. Elemental analyses were in good agreement with the calculated ones. Triply distilled water and AnalaR grade chemicals were used for the syntheses and solution preparations.

Electrochemical Procedures. The electrochemical equipment consisted of a PAR Model 373 potentiostat and IEC F533 function generator for linear potential sweep voltammetry, CV, with output to a Bryans 26000 A-4 X-Y recorder and a Fluke 8000A digital multimeter. A Metrohm using with two kinds of working electrodes: a 1.2-cm^3 Au electrode for CV and a 34-cm^2 platinum screen for preparative work. The coiled platinum-wire counterelectrode was separated by an agar (2 mol dm^{-3} KCl) bridge, and the Ag–AgCl (3 mol dm^{-3} KCl) reference electrode was connected by a Luggin capillary also containing agar (2 mol dm^{-3} KCl). Unless otherwise stated, all potential measurements in this paper will be given vs. the Ag–AgCl reference at 22 ± 2 °C. The working electrode area was determined by cyclic voltammetry in a ferrocyanide solution and calculated with use of the Randless–Ševčik equation.[12] Blank experiments with the supporting electrolyte were performed under the same experimental conditions.

Spectroscopic Measurements. The UV and visible spectra were measured with use of Cary 17 and Varian spectrophotometers. Kinetic runs, using the spectrophotometer, were carried out at room temperature, 22 ± 2 °C. For very long runs the temperature variation was larger.

X-ray Crystal Structure Determination. Crystal data: $Ni(C_{16}H_{36}N_4)(H_2PO_4^-)_2(ClO_4^-)$, mol wt 636.63, triclinic, a = 11.074 (3) Å, b = 9.386 (2) Å, c = 14.299 (2) Å, α = 88.55 (1)°, β = 106.33 (2)°, γ = 111.46 (2)°, $V = 1322.4 \times 10^{-24}$ cm^3, $F(000)$ = 664, μ(Mo Kα) = 9.48 cm^{-1}, ρ_{calcd} = 1.60 g cm^{-3}, ρ_{obsd} = 1.65 g cm^{-3} (by flotation in mixtures of CCl_4 and CH_2I_2), Z = 2, space group $P\bar{1}$ (C_i^1, No. 2) (Mo Kα, λ = 0.709 26 Å). The above lattice constants were determined from diffractometer settings of 15 reflections having $20.1 < 2\theta < 33.0°$.

Collection and Reduction of Diffractometer Data. Intensity data were collected on a crystal grown with use of methods described in the preparation of $Ni^{III}L(H_2PO_4)_2^+$. Unique reflections to a 2θ limit of 54° were measured on a Syntex $P\bar{1}$ diffractometer with a moving-crystal, moving-counter technique and a scan rate that varied between 2 and 24° min^{-1}, depending upon the intensity of the reflection, and scan range (deg) from Mo Kα_1 − 1.0 to Mo Kα_2 + 1.0. Intensities of three standards measured every 60 reflections showed no significant variation during data collection. After correction for instrumental variations and Lp factors, 4282 of 5321 unique reflections had $I >$

(1) (a) Ben Gurion University of the Negev. (b) University of Rhode Island. (c) Nuclear Research Centre Negev.
(2) (a) Olson, D. C.; Vasilevskis, J. *Inorg. Chem.* **1969**, *8*, 1611. (b) Lovechio, F. V.; Gore, E. S.; Busch, D. H. *J. Am. Chem. Soc.* **1974**, *96*, 3109.
(3) Busch, D. H. *Acc. Chem. Res.* **1978**, *11*, 392.
(4) Lati, J.; Meyerstein, D. *Inorg. Chem.* **1972**, *11*, 2393, 2397.
(5) Lati, J.; Meyerstein, D. *Int. J. Radiat. Phys. Chem.* **1975**, *7*, 611. Lati, J.; Koresh, J.; Meyerstein, D. *Chem. Phys. Lett.* **1975**, *33*, 386.
(6) Lappin, A. G.; Murray, C. K.; Margerum, D. W. *Inorg. Chem.* **1978**, *17*, 1630.
(7) Jaacobi, M.; Meyerstein, D.; Lilie, J. *Inorg. Chem.* **1979**, *18*, 429.
(8) Ferraudi, G.; Patterson, L. *J. Chem. Soc., Chem. Commun.* **1977**, 755.
(9) Maruthamuthu, P.; Patterson, L.; Ferrundi, G. *Inorg. Chem.* **1978**, *17*, 1630.
(10) Cohen, H.; Kirschenbaum, L. J.; Zeigerson, E.; Jaacobi, M.; Fuchs, E.; Ginzburg, G.; Meyerstein, D. *Inorg. Chem.* **1979**, *18*, 2763.
(11) Zeigerson, E.; Ginzburg, G.; Shwartz, N.; Luz, Z.; Meyerstein, D. *J. Chem. Soc., Chem. Commun.* **1979**, 241.
(12) Adams, R. N. "Electrochemistry at Solid Electrodes"; Marcel Dekker: New York, 1969; Chapter 5.

0020-1669/82/1321-0073$01.25/0

$3\sigma(I)$ and were considered observed. No corrections were made for absorption.

Solution and Refinement of the Structure. The space group $P\bar{1}$ was selected and later shown to be correct by the successful solution and refinement of the structure. The structure was solved by the heavy-atom method. The positions of the two Ni atoms were determined from the solution of the three-dimensional Patterson function to be on two independent crystallographic centers of symmetry. The scattering factor for the Ni^{III} has been taken from ref 13a. The application of the program SHELX 76[13b] gave a difference map that showed the nitrogen atoms, and subsequent difference Fourier maps revealed the approximate positions of all remaining nonhydrogen atoms. The trial structure based on these coordinates yielded an R of 0.215 for $\sin\theta < 0.2$. The refinement using the SHELX program was continued in stages. Individual isotropic temperature factors were included; the structure was then divided into three blocks corresponding to the two independent molecules, and the ClO_4^-, and the anisotropic refinement of all heavy atoms yielded a discrepancy index of 0.059 for $\sin\theta < 0.45$. Several difference Fourier maps revealed the positions of all of the hydrogen atoms, following which the structure was divided into five blocks and was refined to convergence with use of anisotropic thermal parameters for the nonhydrogen atoms and isotropic thermal parameters for hydrogens with a conventional R of 0.046 (0.058 including nonobserveds), a weighted R_w of 0.051, and goodness of fit of 1.04. A final difference Fourier map revealed no peaks of chemical significance.

Results and Discussion

Preparation and Characterization of NiL^{3+}. In cyclic voltammograms of solutions containing NiL^{2+} in 0.3 M $NaClO_4$ at pH 2.0, no oxidation wave is observed. However the current at potentials ≥ 0.95 V is considerably larger than that observed in blank solutions. Furthermore, when the cyclic voltammogram was extended to 1.1 V, a reduction wave with a peak at 0.96 V was observed during the backward scan. The current of this reduction wave is considerably smaller than that of the integrated anodic current. These results indicate that an unstable oxidized product, identified below as NiL^{3+}, is formed and the redox potential for the couple NiL^{3+}/NiL^{2+} is estimated as ≥ 0.98 V.

In preparative electrochemical experiments at 1.25 V solutions containing 5×10^{-4} M $NiL(ClO_4)_2$ in 0.3 M $NaClO_4$ at pH 2.0 turned light green. The absorption spectrum of such a solution is given in Figure 1. As the product is short-lived, the spectrum was measured by fast forward and backward scans. The molar absorption coefficients were determined by quenching experiments in which equal amounts of the test solution were mixed with 0.2 M Na_2SO_4 at pH 2.0 at the moment of measuring the absorption of an identical solution. This quenching experiment yields a solution with a spectrum identical with that of $Ni^{III}L(SO_4)_2^-$. (For the identification of the product as $Ni^{III}L(SO_4)_2^-$ and not as $Ni^{III}LSO_4^+$, as earlier suggested,[10] see below.) The formation of the $Ni^{III}L(SO_4)_2^-$ complex by the addition of sulfate proves that the electrochemical oxidation product is a tervalent nickel complex, most probably $NiL(H_2O)_2^{3+}$.

The spectrum of $NiL(H_2O)_2^{3+}$ (Figure 1), $\lambda_{max} = 395$ nm, $\epsilon_{395} = 4300 \pm 1000$ M^{-1} cm^{-1}, and a shoulder at $\lambda = 325$ nm, $\epsilon_{325} = 3300 \pm 800$ M^{-1} cm^{-1}, differs in nature from that reported[9,10] for NiL^{3+} formed in the reaction

$$NiL^{2+} + OH \rightarrow NiL^{3+} \qquad (2)$$

at pH 3.0. At this pH over 80% of the complex is in the form of NiL^{3+} and less than 20% in the form of $Ni^{III}L(OH)^{2+}$ as the pK_a is 3.7 for this process.[10] One possible explanation for the discrepancy between the spectra of NiL^{3+} obtained by the two techniques is that whereas reaction 2 is diffusion controlled[10] and clearly proceeds without a configurational change of the ligand, the electrochemical oxidation process in the perchlorate solutions is very slow and highly irreversible[14] and might involve such a configurational change. It should be noted that the spectra of both forms of NiL^{3+} differ considerably from those of $Ni^{III}LX_n$, where X is a stabilizing anion and $n = 2$ or 1 (see below). Also this observation supports earlier suggestions that the configuration of the ligands around tervalent nickel with macrocyclic ligands considerably affects the nature of the absorption spectra of the complexes.[10]

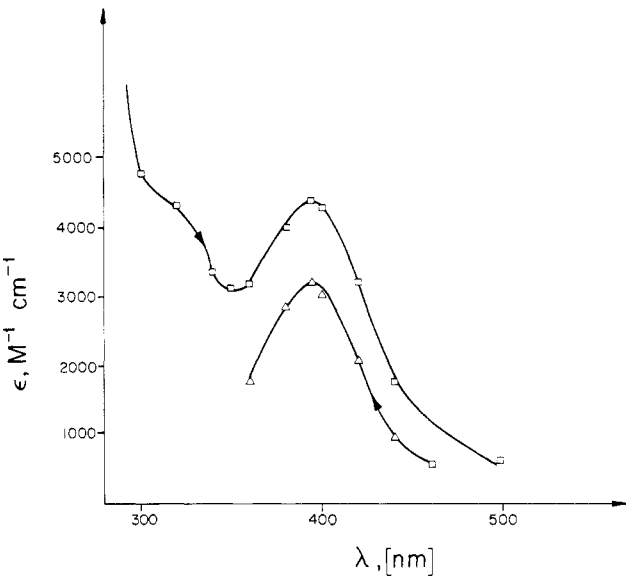

Figure 1. UV–vis absorption spectrum of $NiL(H_2O)_2^{3+}$ in 0.3 M $NaClO_4$ at pH 2.0, a short time after its electrochemical preparation. Arrows indicate the scan direction. Absorption coefficients are for the upper curve. Lower curve indicates the degree of decomposition within ca. 30 s.

The kinetics of decomposition of the electrochemically formed $Ni^{III}L(H_2O)_2^{3+}$ was followed. It was found that the kinetics does not obey a simple first- or second-order rate law. The half-life of $Ni^{III}L(H_2O)_2^{3+}$ at pH 2.0 in solutions containing ca. 1×10^{-4} M of the tervalent complex is 1.2 ± 0.2 min.

Preparative electrochemical oxidation of NiL^{2+} in 0.1 M $NaClO_4$ at a starting pH of 3.2 yielded a very short-lived pink solution, which upon quenching with an acidic Na_2SO_4 solution yielded a solution containing $Ni^{III}L(SO_4)_2^-$. The pink solution probably contains $Ni^{III}LOH^{2+}$ or NiL^{3+} in the same configuration as that formed in reaction 2.[10,15]

Stabilization of $Ni^{III}L$ by Axial Coordination of Sulfate. The equilibrium constant of reaction 1 was shown to be $K_1 = 3 \times 10^3$ M^{-1} at $\mu = 0.3$ by two independent techniques.[10] However the redox potential of $Ni^{III}L/Ni^{II}L$ in 0.5 M sulfate solutions is 0.64 V[14b] (Table I); i.e., it is more than 0.34 V less positive than that observed in perchlorate-containing solutions.[10,11,14] If reaction 1 is the only process affecting the redox potential,

(13) (a) "International Tables for X-ray Crystallography"; Kynoch Press: Birmingham, England, 1974; Vol. IV, p 99. (b) Sheldrick, G. M. "SHELX, A Programme for Crystal Structure Determination", University of Cambridge, 1976.

(14) (a) Zeigerson, E.; Ginzburg, G.; Kirschenbaum, L. J.; Meyerstein, D. *J. Electroanal. Chem. Interfacial Electrochem.*, in press. (b) The CV of $Ni^{II}L$ in 0.5 M Na_2SO_4 indicates a reversible electrochemical redox process. A detailed analysis of the electrochemistry of Ni^{II} in Na_2SO_4 and $NaClO_4$ is given in ref 14a.

(15) The red form of NiL^{3+} has also been attributed to the metal-stabilized free radical[16,17]

however due to arguments outlined earlier in detail we prefer to identify it as $NiLOH^{2+}$.[10]

(16) Barefield, E. K.; Mocella, M. T. *J. Am. Chem. Soc.* **1975**, *97*, 4238.

(17) Whitburn, K. D.; Laurence, G. S. *J. Chem. Soc., Dalton Trans.* **1979**, 139.

Table I. Properties of $Ni^{III}LX_2$ Complexes in Slightly Acidic Aqueous Solutions[a]

axial ligand X	[X], M	pH	redox potential, V (vs. Ag/AgCl)	stability const for ligation of X	half-life for dec of $Ni^{III}LX_2$[b]	abs spectrum, λ, nm (ε, M^{-1} cm^{-1})
H_2O		2.0	~0.98		~1.2 min	325 sh (3300), 395 (4300)[c]
Cl^-	0.3	2.0	...	~250 M^{-2} [d]	75 min	315 (9400), 400 sh (5000)[c]
$H_2PO_4^-$	0.3	2.0	0.72	>10^4 M^{-2},[e] ~2×10^4 M^{-2},[d] ~5×10^6 M^{-2} [d,f]	4 days	280 (8000), 385 (7500), 730 (50)
SO_4^{2-}	0.5	2.0	0.64	~5×10^6 M^{-2},[e] 3×10^3 M^{-1},[d,f] >5×10^5 M^{-2} [d,g]	>1 year	310 (11 000), 410 (7000), 710 (60)
$C_8H_4O_4^{2-}$	0.3	4.2	0.57	≥10^7 M^{-2} [e]	12 days[h]	310 (12 400), 400 (6800)[c]

[a] The solutions probably contain a mixture of $Ni^{III}LX_2$ and $Ni^{III}LX$. [b] Approximate values measured for solutions containing ca. 3×10^{-4} M $Ni^{III}LX_2$ + $Ni^{III}LX$. The approximation stems from the fact that the decomposition reaction does not obey a pure first- or second-order rate law (see text). [c] The concentration of the solutions was too small for measuring the absorption band at λ > 600 nm. However the solutions were green, indicating the existence of an absorption band in this region. [d] Calculated from the rate of decomposition of $Ni^{III}LX_2$ and/or from the effect of [X] on the absorption of $Ni^{III}LX_2$ (see text). [e] Calculated from the redox potential with the assumption that $Ni^{III}LX_2$ and not $Ni^{III}LX$ is formed. No correction for activity constants was introduced. [f] K_1 was obtained by the pulse radiolytic technique.[10] [g] From the rate of decomposition of $Ni^{III}L(SO_4)_2^-$ as a function of [SO_4^{2-}], with the assumption that only $NiL(H_2O)_2^{3+}$ decomposes and not $NiLSO_4^+$ or $NiL(SO_4)_2^-$. [h] Measured at pH 4.2. In a solution containing 0.3 M SO_4^{2-} at the same pH, $t_{1/2}$ = 1.5 days.

then the $K_1 \sim 10^6$ M^{-1} would be predicted from the electrochemical results. The result can be explained if a second equilibrium occurs in sulfate solutions:

$$Ni^{III}LSO_4^+ + SO_4^{2-} \rightleftharpoons Ni^{III}L(SO_4)_2^- \qquad K_3 \sim 10^3\ M^{-1} \tag{3}$$

The conclusion that the major species in 0.1 M sulfate solutions is $Ni^{III}L(SO_4)_2^-$ explains also the large effect of sulfate on the lifetime of the tervalent nickel complex. Also in solutions containing very low concentrations of sulfate, where the kinetics of decomposition obeyed a rate law that is between first and second order in tervalent nickel, the effect of sulfate is larger than predicted from K_1 only (Table II).

It should be noted that the pulse radiolytic experiments[10] were carried out under conditions of low sulfate concentrations in order to obtain maximal accuracy in the determination of K_1. Thus if the absorption spectrum of $Ni^{III}L(SO_4)_2^-$ does not differ considerably from that of $Ni^{III}LSO_4^+$, equilibrium 3 does not affect the determination of K_1 and its presence would not be observed.

Further evidence for the role of sulfate in stabilizing $Ni^{III}L^{3+}$ was obtained from the following experiments: (a) To a solution containing $Ni^{III}L(SO_4)_2^-$ in 0.1 M Na_2SO_4 at pH 1.6 was added a saturated $Ba(NO_3)_2$ solution. The green color due to $Ni^{III}L$ disappeared within less than 5 min. (b) To a solution containing $Ni^{III}L(SO_4)_2^-$ in 0.1 M Na_2SO_4 at pH 3.8 was added a saturated $Ba(NO_3)_2$ solution at pH 8.9. A very short-lived red intermediate was observed under these conditions, and the final pH was 5.5. (c) Finally if the latter red solution is quickly quenched with an acidic concentrated sulfate solution, the green color due to $Ni^{III}L(SO_4)_2^-$ is restored.

A saturated solution containing 2×10^{-3} M $Ni^{II}L(ClO_4)$ in 0.1 M H_2SO_4 was quantitatively oxidized electrochemically. This solution was saturated again with $Ni^{II}L(ClO_4)_2$ and the process repeated until a solution containing 8×10^{-3} M $Ni^{III}L(SO_4)_2^-$ was obtained. Upon addition of $HClO_4$ to this solution a deep green solid precipitated. Dissolution of this solid in 0.1 M H_2SO_4 yielded a solution with the spectrum of $Ni^{III}L(SO_4)_2^-$, and from the measured absorption a molecular weight of 540 ± 20 was calculated for the solid. This result indicates that the solid is either $[Ni^{III}LSO_4]ClO_4$, mol wt 538.5, or $[NiL(SO_4)(H_2O)]ClO_4$, mol wt 556.5. We prefer the latter assignment as the green color is believed to indicate an octahedral ligation of the tervalent nickel.

The IR spectra of $[Ni^{II}L](ClO_4)_2$ and $[Ni^{III}L(SO_4)(H_2O)]ClO_4$ were measured both in Nujol and as a Br pellet. The only significant difference observed between the two compounds is that the N–H stretching frequency is shifted from 3180 cm^{-1} in the divalent complex to 3080 cm^{-1} in the tervalent one. This shift is in agreement with our expectation and with the reported spectrum of $Ni^{III}L(CH_3CN)_2(ClO_4)_3$.[1]

Table II. Stabilization of $Ni^{III}L$ in Solutions Containing Chloride, Sulfate, and Their Mixtures[a]

[SO_4^{2-}], M	[Cl^-], M	[ClO_4^-], M	$t_{1/2}$, min
0	0	0.30	1.2
0	0.15	0.15	15
0	0.25	0.05	65
0	0.30	0	75
0.0005	0	0.30	25
0	0.15	0.15	15
0.0005	0.15	0.15	35
0.0010	0.15	0.147	90
0.0015	0.15	0.144	110
0.0030	0.15	0.141	250
0.0050	0.15	0.135	~400
0.050	0.15	0	>weeks
0.0024	0	0.30	225
0.0024	0.05	0.25	90
0.0024	0.10	0.20	100
0.0024	0.20	0.10	120
0.0024	0.25	0.05	230

[a] $[Ni^{III}LX_n]_0 = 3 \times 10^{-4}$ M, pH 2.0, μ = 0.3 M.

Stabilization of $Ni^{III}L$ by Axial Coordination of Other Anions. Cyclic voltammograms of $Ni^{II}L$ in solutions containing 0.3 M NaCl or 0.3 M NaH_2PO_4 at pH 2.0 and 0.3 M sodium phthalate at pH 4.0 are plotted in Figure 2. (The concentration of $Ni^{II}L$ in the latter solution is only 1×10^{-4} M due to solubility limitations.) The results clearly indicate that the anions of these salts, like sulfate, affect the electrochemical oxidation of $Ni^{II}L$. The results indicate that the electrochemical oxidation in the presence of phosphate and phthalate is reversible and that the redox potential of the $Ni^{III}L/Ni^{II}L$ couple in these media is considerably lower than that in solutions containing perchlorate as the supporting electrolyte. The oxidation of $Ni^{II}L$ in the chloride-containing solution occurs in the same voltage range as the oxidation of chloride (Figure 2). However the backward scan in the latter solution clearly indicates that in the presence of $Ni^{II}L$ at least one additional oxidation product is formed.

Preparative electrochemical oxidation of $Ni^{II}L$ in the phosphate-, phthalate-, and chloride-containing media yielded green solutions. The spectroscopic and electrochemical data thus obtained as well as the half-lives of the tervalent nickel complex in the different media are summed up in Table I. The molar absorption coefficients were obtained from coulometric determinations of the concentration of the $Ni^{III}L$ in the

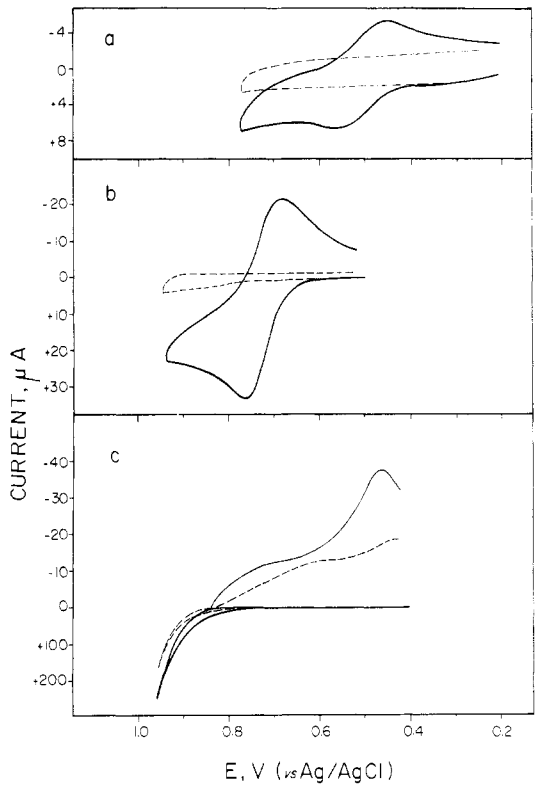

Figure 2. Cyclic voltammograms of $NiL(ClO_4)_2$ in different media with a 1.2-cm^2 Au anode and a scan rate of 11.2 mV s^{-1}. Dashed lines represent the supporting electrolyte only: (a) 0.3 M sodium phthalate, 8×10^{-5} M NiL^{2+}, pH 4.0; (b) 0.3 M sodium phosphate, 5×10^{-4} M NiL^{2+}, pH 2.0; (c) 0.3 M sodium chloride, 5×10^{-4} M NiL^{2+}, pH 2.0.

phosphate- and phthalate-containing media and by addition of high concentrations of Na_2SO_4 and determining the concentration of $Ni^{III}L(SO_4)_2^-$ in the chloride and phosphate media. The stability constants for axial complexation were calculated from the electrochemical data and from the kinetic stabilizing effect of the ligand as determined from the rate of decomposition of $Ni^{III}LX_2$. The reasons for assuming that the complexes are mainly $Ni^{III}LX_2$ and not $Li^{III}LXH_2O$ or $Ni^{III}LX$ are discussed below.

$Ni^{III}L(C_8H_4O_4)_2^-$

The measured redox potential for the $Ni^{III}L/Ni^{II}L$ couple in phthalate solutions, 0.57 V, is the lowest observed in this study, indicating a high stability constant for axial ligation. We believe that the ligand is $C_8H_4O_2^{2-}$ though $C_8H_5O_4^-$ cannot be definitely ruled out. However as the pH of the solutions is ca. 4.0, i.e., near the second pK of phthalic acid, and the tervalent nickel is expected to increase its acidity, the assumption that the ligand is $C_8H_4O_2^{2-}$ seems more reasonable.

The half-life for the decomposition of $Ni^{III}L(C_8H_4O_4)_2^-$ in solutions containing 0.3 M sodium phthalate at pH 4.2 is ca. 12 days. For comparison we note that $t_{1/2}$ for the decomposition of $Ni^{III}L(SO_4)_2^-$ and $Ni^{III}L(HPO_4)_2^-$ in solutions containing 0.3 M sulfate or phosphate at the same pH is 1.5 days and 3.2 h, respectively. This result also indicates the very high stability constant of the $Ni^{III}L(C_8H_4O_2)_2^-$ complex even at pHs higher than that of the pK for the reaction

$$Ni^{III}L(H_2O)_2^{3+} \rightleftharpoons Ni^{III}LOH^{2+} \qquad pK = 3.7^{10} \qquad (4)$$

$Ni^{III}LCl_2^+$

As the cyclic voltammogram of $Ni^{II}L$ in chloride media is far from reversible (Figure 2), we could not determine the stability constant for chloride complexation from the electrochemical data. We tried to estimate this stability constant from a spectrophotometric titration. The largest difference in the molar absorption coefficients of $Ni^{III}L$ in sulfate and chloride media is at 420 nm, where $\epsilon(Ni^{III}L)$ equals 6900 and 4800 M^{-1} cm^{-1}, respectively. Different sulfate concentrations were added to a $Ni^{III}L$ solution in a 0.15 M NaCl solution at pH 2.0. A molar absorption coefficient of 5850 M^{-1} cm^{-1} was obtained for the solution containing 1.0×10^{-3} M Na_2SO_4. From this result and by assuming $K_{SO_4^{2-}} = [NiL(SO_4)_2^-]/[NiL^{3+}][SO_4^{2-}]^2 \simeq 5 \times 10^6$ M^{-2}, we calculate $K_{Cl^-} = [Ni^{III}LCl_2^+]/[NiL^{3+}][Cl^-] \approx 250$ M^{-2}. (In this calculation the role of $Ni^{III}LCl^{2+}$ and $Ni^{III}LClSO_4$ was neglected.) Axial ligation of chloride to the tervalent nickel cyclam complex was recently reported.[18]

The kinetics of decomposition of $Ni^{III}L$ in chloride-containing solutions was followed. The rate law observed was always somewhere between first and second order. In Table II are reported the half-lives observed under different conditions in solutions containing 3×10^{-4} M $Ni^{III}LX_n$. Three series of experiments are reported:

a. The effect of chloride concentration at constant ionic strength was investigated. These results indicate that the lifetime of $Ni^{III}L$ increases somewhat more than with a second-order dependence on $[Cl^-]$, in agreement with the assumption that $Ni^{III}Cl_2^+$ is the major component at high chloride concentrations.

b. The addition of sulfate to chloride-containing solutions at constant ionic strength increases considerably the lifetime of $Ni^{III}L$, as expected.

c. Addition of low concentrations of chloride to a solution containing a low concentration of sulfate shortens the lifetime of $Ni^{III}L$. However addition of higher chloride concentrations increases the lifetime of $Ni^{III}L$. As the addition of chloride can only decrease the concentration of NiL^{3+}, this result indicates that $Ni^{III}LCl^{2+}$, or $[Ni^{III}LClH_2O]^{2+}$, has a shorter lifetime than $Ni^{III}LSO_4^+$, $Ni^{III}L(SO_4)_2^-$, and $Ni^{III}LCl_2^+$.

$Ni^{III}L(H_2PO_4)_2^+$ and $Ni^{III}L(HPO_4)_2^-$

Preparative electrolysis at +900 mV of a solution containing 0.3 M NaH_2PO_4 at pH 2.4 that was saturated consecutively three times with $NiL(ClO_4)_2$ yielded a dark green solution containing ca. 9×10^{-3} M $Ni^{III}L(H_2PO_4)_2^+$ (for the identification see below). This solution was further concentrated by vacuum evaporation at room temperature and then several drops of 3 M $NaClO_4$ were added, and the solution was refrigerated for several days at 4 °C. Dark green crystals precipitated from this solution.

The X-ray crystal structure determination of this compound is described in the Experimental Section. Final coordinates are given in Table III.[19] Molecule A is the one centered on the origin, while molecule B is located at $0,{}^1/_2,{}^1/_2$. Two views of molecule A are given in Figure 3. Primed atoms are those obtained via inversion.

Bond lengths and bond angles are given in Tables IV and V. In general chemically equivalent derived parameters are in agreement between the two crystallographically independent molecules, except for geometric features which include Ni and the phosphate group, where experimentally significant differences are observed. However, the esd's of the parameters involving Ni are underestimated by at least a factor of 1.4 since the atoms are located on crystallographic special positions and the positional parameters are not refined. The atom numbering for the $H_2PO_4^-$ moiety has been chosen such that O(4) is the axial atomic ligand and O(3) is bonded only to P.

The Ni^{III}–N distances found here are in the range found also for Ni^{II}–N in saturated macrocyclic hexacoordinated

(18) Haines, R. I.; McAuley, A. *Inorg. Chem.* **1980**, *19*, 719.
(19) Thermal parameters and a listing of structure factor amplitudes appear in the supplementary material.

Table III. Atomic Coordinates ($\times 10^4$ for Nonhydrogen Atoms, $\times 10^3$ for Hydrogen Atoms)

	molecule A			molecule B		
	x	*y*	*z*	*x*	*y*	*z*
Ni	0000	0000	0000	0000	5000	5000
P	−0546 (1)	0729 (1)	2151 (1)	1329 (1)	4570 (1)	7454 (1)
O(1)	−0322 (4)	−0301 (3)	3007 (2)	2895 (3)	5087 (4)	7980 (2)
O(2)	−2116 (3)	0108 (5)	1586 (2)	0540 (3)	2999 (3)	7469 (2)
O(3)	−0097 (3)	2328 (3)	2576 (2)	0941 (4)	5596 (4)	8130 (2)
O(4)	0107 (3)	0536 (3)	1408 (2)	1152 (2)	5233 (3)	6449 (2)
N(1)	0767 (3)	2226 (3)	−0199 (2)	0963 (3)	3837 (3)	4567 (2)
C(2)	−0355 (4)	2795 (4)	−0335 (3)	0528 (4)	2296 (4)	4943 (2)
C(3)	−1617 (4)	1599 (4)	−0966 (3)	−0971 (4)	1762 (4)	4772 (3)
N(4)	−1846 (3)	0144 (3)	−0473 (2)	−1220 (3)	2954 (3)	5274 (2)
C(5)	−3173 (4)	−1172 (4)	−0989 (3)	−2685 (3)	2560 (4)	5216 (2)
C(6)	−3160 (4)	−2624 (5)	−0495 (3)	−2774 (4)	3912 (4)	5739 (3)
C(7)	−2064 (4)	−3200 (4)	−0535 (2)	−2450 (4)	5427 (4)	5272 (3)
C(8)	−4342 (5)	−0795 (7)	−0823 (4)	−3109 (5)	1151 (5)	5802 (4)
C(9)	−3348 (5)	−1362 (6)	−2082 (3)	−3599 (4)	2217 (5)	4162 (3)
C(10)	−2479 (6)	−4895 (5)	−0350 (4)	−2981 (5)	6460 (5)	5716 (4)
H(1)	092 (3)	222 (4)	−078 (3)	060 (4)	364 (4)	393 (3)
H(2)	−047 (3)	291 (4)	031 (3)	113 (4)	239 (5)	564 (3)
H(2)	−024 (4)	363 (5)	−065 (3)	081 (4)	167 (4)	461 (3)
H(3)	−237 (4)	188 (5)	−109 (3)	−142 (4)	081 (5)	499 (3)
H(3)	−156 (4)	144 (5)	−157 (3)	−139 (4)	162 (5)	408 (3)
H(4)	−198 (4)	036 (5)	007 (3)	−077 (4)	308 (4)	592 (3)
H(6)	−314 (4)	−252 (4)	028 (3)	−220 (4)	409 (4)	637 (3)
H(6)	−396 (5)	329 (6)	−076 (3)	−363 (5)	362 (6)	590 (4)
H(7)	−176 (4)	−293 (5)	−116 (3)	−277 (4)	541 (5)	462 (3)
H(8)	−504 (6)	−156 (7)	−104 (4)	−306 (5)	023 (7)	542 (4)
H(8)	−435 (4)	020 (5)	−114 (3)	−239 (5)	144 (5)	647 (3)
H(8)	−431 (5)	−086 (6)	−010 (4)	−396 (5)	089 (6)	581 (3)
H(9)	−422 (6)	−223 (7)	−241 (4)	−371 (4)	100 (5)	390 (3)
H(9)	−254 (4)	−144 (4)	−215 (3)	−454 (4)	227 (5)	416 (3)
H(9)	−354 (4)	−044 (6)	−233 (3)	−332 (4)	295 (5)	370 (3)
H(10)	−325 (5)	−541 (6)	−082 (4)	−388 (4)	598 (5)	570 (3)
H(10)	−175 (9)	−503 (10)	−029 (6)	−287 (5)	732 (6)	539 (4)
H(10)	−262 (6)	−499 (7)	048 (5)	−237 (5)	665 (6)	643 (4)
HO(1)	020 (8)	−051 (10)	317 (6)	320 (6)	452 (8)	784 (5)
HO(2)	−234 (6)	081 (7)	199 (5)	080 (6)	371 (7)	795 (4)

ClO_4^-

	x	*y*	*z*		*x*	*y*	*z*
Cl	4479 (1)	2591 (1)	7248 (1)	O(7)	4009 (6)	2602 (8)	8062 (5)
O(5)	5761 (4)	2518 (7)	7548 (3)	O(8)	4670 (9)	4100 (8)	6965 (6)
O(6)	3649 (7)	1600 (10)	6497 (7)				

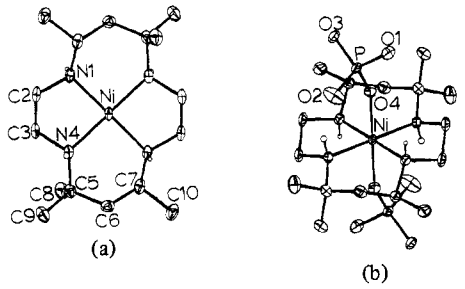

Figure 3. (a) ORTEP view on the plane of the macrocycle of molecule A, including atomic numbering. The axial dihydrogen phosphate ligands have been eliminated for clarity. Molecule B is essentially identical with this view. (b) Rotation of view a by ca. 30° about the horizontal axis, with the two centrosymmetrically related axial dihydrogen phosphate ligands included. In both views hydrogens, except those on the nitrogens, have been omitted for clarity. Ellipsoids are drawn at the 30% probability level.

Table IV. Bond Distances (Å) in $NiL(H_2PO_4)_2ClO_4$

	molecule A	molecule B
Ni-O(4)	2.048 (3)	2.074 (3)
Ni-N(1)	1.994 (3)	1.992 (3)
Ni-N(4)	2.019 (3)	2.007 (3)
P-O(1)	1.562 (3)	1.585 (3)
P-O(2)	1.584 (3)	1.493 (3)
P-O(3)	1.483 (3)	1.557 (3)
P-O(4)	1.491 (3)	1.504 (3)
N(1)-C(2)	1.487 (5)	1.486 (4)
C(2)-C(3)	1.491 (5)	1.495 (6)
C(3)-N(4)	1.492 (5)	1.490 (4)
N(4)-C(5)	1.529 (5)	1.504 (4)
C(5)-C(6)	1.522 (6)	1.536 (5)
C(5)-C(8)	1.539 (6)	1.543 (6)
C(5)-C(9)	1.527 (6)	1.526 (5)
C(6)-C(7)	1.513 (6)	1.520 (5)
C(7)-C(10)	1.525 (6)	1.532 (6)
C(7)-N(1′)	1.497 (4)	1.485 (5)

ClO_4^-

Cl-O(5)	1.390 (4)	Cl-O(7)	1.404 (7)
Cl-O(6)	1.316 (9)	Cl-O(8)	1.419 (7)

complexes[20,21] and are slightly longer than those in unsaturated complexes.[22,23] Martin et al.[24] have suggested that a typical value for Ni^{II}–N in high-spin macrocyclic complexes is 2.13 Å, while the distance may be shortened to as low as 1.86 Å

(20) Bosnich, B.; Mason, R.; Pauling, P. J.; Robertson, G. B.; Tobe, M. L. *Chem. Commun.* **1965**, 97.
(21) (a) Curtis, N. F.; Swann, D. A.; Waters, T. N. *J. Chem. Soc., Dalton Trans.* **1973**, 1408, 1963. (b) Bosnich, B.; Mason, R.; Pauling, P. J.; Robertson, G. B.; Tobe, M. L. *J. Chem. Soc., Chem. Commun.* **1965**, 97.
(22) Hanic, F.; Miklos, D. *J. Cryst. Mol. Struct.* **1972**, *2*, 115.
(23) Bailey, M. F.; Maxwell, I. E. *J. Chem. Soc., Dalton Trans.* **1972**, 938.

Table V. Bond Angles (Deg) in $NiL(H_2PO_4)_2ClO_4$

	molecule A	molecule B
N(1)-Ni-O(4)	90.5 (1)	92.7 (1)
P-O(4)-Ni	150.9 (2)	149.7 (2)
C(2)-N(1)-Ni	106.3 (2)	107.0 (2)
C(5)-N(4)-Ni	125.7 (2)	124.1 (2)
O(3)-P-O(1)	108.3 (2)	102.2 (2)
O(3)-P-O(2)	109.9 (2)	108.4 (2)
O(4)-P-O(3)	115.2 (2)	111.0 (2)
N(4)-C(3)-C(2)	107.6 (3)	107.0 (3)
C(6)-C(5)-N(4)	107.8 (3)	107.6 (3)
C(9)-C(5)-N(4)	111.1 (3)	112.1 (3)
C(9)-C(5)-C(6)	111.8 (3)	111.5 (3)
C(9)-C(5)-C(8)	110.3 (4)	110.5 (3)
N(4)-Ni-O(4)	89.8 (1)	87.0 (1)
N(4)-Ni-N(1)	86.9 (1)	85.9 (1)
C(3)-N(4)-Ni	104.8 (2)	106.6 (2)
O(2)-P-O(1)	108.0 (2)	111.0 (2)
O(4)-P-O(1)	110.8 (2)	109.2 (1)
O(4)-P-O(2)	104.5 (2)	114.4 (2)
C(3)-C(2)-N(1)	107.8 (3)	106.9 (3)
C(5)-N(4)-C(3)	114.1 (3)	114.0 (3)
C(8)-C(5)-N(4)	107.6 (3)	107.5 (3)
C(8)-C(5)-C(6)	108.1 (4)	107.5 (3)
C(7)-C(6)-C(5)	117.8 (3)	117.2 (3)
C(10)-C(7)-C(6)	110.4 (4)	108.9 (3)
N(1')-Ni-O(4)	89.5 (1)	87.3 (1)
N(4')-Ni-N(1)	93.1 (1)	94.1 (1)
C(7)-N(1')-Ni	117.2 (2)	119.3 (2)
N(4')-Ni-O(4)	90.2 (1)	93.0 (1)
N(1')-C(7)-C(10)	112.0 (3)	111.3 (2)
N(1')-C(7)-C(6)	108.4 (3)	109.5 (3)
ClO_4^-		
O(6)-Cl-O(5) 112.8 (4)	O(7)-Cl-O(5)	109.8 (3)
O(8)-Cl-O(5) 106.1 (4)	O(7)-Cl-O(6)	117.0 (4)
O(8)-Cl-O(6) 108.7 (5)	O(8)-Cl-O(7)	101.1 (4)

in low-spin complexes,[25] which is close to the values obtained here for Ni^{III}–N.

The bond angles also exhibit a pattern that appears to be fairly consistent for most nickel macrocycles. The N–Ni–N angle contained in the five-membered ring is generally less than 90° while that in the six-membered ring tends to be greater than 90°.[23] A similar pattern is observed in the isoelectronic low-spin Co(II) structures reported by Endicott et al.[26]

The presence of the Ni ions on crystallographic centers of symmetry requires strict coplanarity of the four nitrogen ligands with the metal. The only other reported cases of a nickel macrocycle with such a restriction are $Ni(\gamma\text{-tet b})(ClO_4)_2$[21a] and Ni(cyclam)$Cl_2$[21b] although a number of Co(II) and Co(III) complexes have a similar geometry.[26] In other cases the distortion is tetrahedral with individual nitrogen atoms deviating up to ±0.18 Å from the best plane of the five central atoms.[27]

Warner and Busch[28] have given a detailed discussion of the factors determining the stabilities of the various possible configurations and conformations of Ni(II) macrocycles containing six asymmetric centers. Their arguments and predictions are relevant to this structure. A comparison of the torsion angles for the two independent molecules in Table VI shows that they differ by an average of 3.3° with the largest difference being 7.2°. While these differences are significantly larger than the standard deviations of the individual torsion angles, they do not suggest any large conformational differences between the two macrocycles. An additional measure of the conformation is the deviation from the best plane of the metal and four nitrogens, which again indicates a similar pattern for the two molecules.

Table VI. Torsion Angles (Deg) of the Macrocycle

atom quartet	molecule A	molecule B
N(4)-Ni-N(1)-C(2)	13.2 (2)	−15.7 (2)
N(1)-Ni-N(4)-C(5)	151.9 (3)	−150.4 (2)
N(1)-Ni-N(4)-C(3)	16.6 (2)	−14.6 (2)
Ni-N(1)-C(2)-C(3)	−41.0 (3)	43.0 (3)
N(1)-C(2)-C(3)-N(4)	57.6 (4)	−56.9 (3)
C(2)-C(3)-N(4)-C(5)	175.2 (3)	−177.2 (3)
Ni-N(4)-C(5)-C(8)	156.1 (3)	−161.0 (3)
C(3)-N(4)-C(5)-C(6)	171.6 (3)	−178.5 (3)
C(3)-N(4)-C(5)-C(9)	48.7 (4)	−55.5 (4)
N(4)-C(5)-C(6)-C(7)	−62.3 (4)	66.7 (4)
C(8)-C(5)-C(6)-C(7)	−178.3 (4)	−177.8 (3)
C(5)-C(6)-C(7)-C(10)	−159.6 (4)	163.8 (3)
Ni-N(4)-C(5)-C(6)	39.8 (4)	−45.5 (3)
Ni-N(4)-C(5)-C(9)	−83.1 (4)	77.4 (3)
C(3)-N(4)-C(5)-C(8)	−72.1 (4)	66.1 (4)

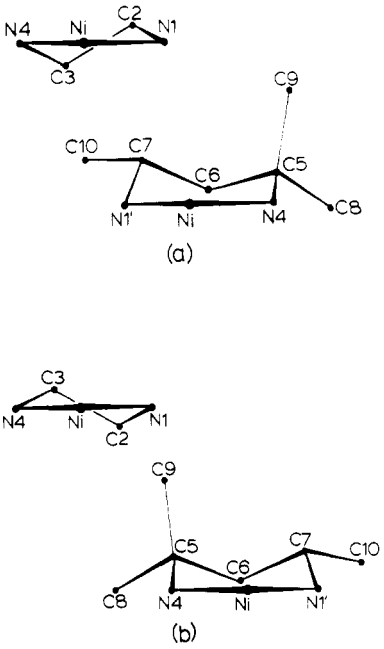

Figure 4. View on a plane normal to the best plane of NiN_4, showing the conformations of the 5- and 6-membered rings: (a) molecule A; (b) molecule B.

Again, by virtue of crystallographic site symmetry the complex is a meso diastereomer, and in accordance with Warner and Busch the six-membered rings have a chair conformation with the methyl groups on asymmetric carbons in the equatorial position, as shown in Figure 4. H1 and H4′ are axial across the "mouth" of the six-membered ring and, as predicted, give rise to a staggered conformation for the five-membered chelate ring, Figure 4b. In the centrosymmetric $[Ni^{II}(\gamma\text{-tet b})](ClO_4)_2$ the five-membered ring is staggered but the six-membered ring adopts a "twist-boat" geometry. Hence this structure corresponds to Figure 4a of ref 28 and appears to be one of the first direct confirmations of the Warner–Busch predictions.

This compound is the second[21b] structure of a ([14]ane-N_4) nickel complex with hexacoordination, and the stoichiometry proves conclusively the existence of a Ni(III) complex. An analogous structural situation, including the location of the metal ion on a center of symmetry, is encountered in low-spin Co^{II}([14]ane-N_4)$(ClO_4)_2$,[26] where the equatorial Co–N bonds are both 1.98 Å while the axial Co–O bonds are 2.41 Å. In the *meso*-([14]ane-N_4)(acac-C)Ni^{II} complex the Ni–O dis-

(24) Martin, L. Y.; Sperati, C. R.; Busch, D. H. *J. Am. Chem. Soc.* **1977**, *99*, 2968.
(25) Waters, J. M.; Whittle, K. R. *J. Inorg. Nucl. Chem.* **1972**, *34*, 155.
(26) Endicott, J. F.; Lilie, J.; Kuszai, J. M.; Ramaswamy, B. S.; Schmonsees, W. G.; Simic, M. G.; Glick, M. D.; Rillema, D. P. *J. Am. Chem. Soc.* **1977**, *99*, 429.
(27) Maxwell, I. E.; Bailey, M. F. *J. Chem. Soc., Dalton Trans.* **1972**, 935.
(28) Warner, L. G.; Busch, D. H. *J. Am. Chem. Soc.* **1969**, *91*, 4092.

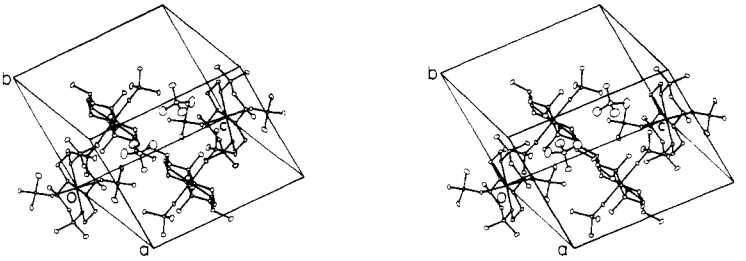

Figure 5. Stereoview of the structure.

tances are 2.05 Å,[21] similar to the values for the two independent molecules (2.05 and 2.07 Å) in the present structure. The shortness of this bond relative to the isoelectronic Co(II) complex suggests a lower Jahn–Teller distortion in the case of Ni(III). The N–Ni–O angles are all very close to 90°, indicating true axial coordination.

The disposition of the $H_2PO_4^-$ ligand is reminiscent of that found in the above-mentioned Co(II) complex (compare Figure 3b with Figure 7a of ref 28). The Ni–O(4)–P angles are 150.9 and 149.7°, but there is no obvious reason for such high values. O(3) is essentially gauche to the Ni in both molecules, the appropriate torsion angles being −113.6 and −98.7° for molecules A and B, respectively. There are no intramolecular hydrogen bonds, the shortest O···N distance being greater than 3.9 Å. Other geometric features of the dihydrogen phosphate group are quite normal.

The structure shown in Figure 5 may be described as infinite chains of cations running along their lines of centers ([011]), while individual chains are isolated from each other by a parallel chain of perchlorate ions. The angle between the normals to the two NiN_4 planes is 141°. There are no hydrogen bonds involving the ClO_4^- moiety, but there does appear to be an intercomplex hydrogen bond between O(1) of molecule A and O(2) of molecule B (related by $\bar{x}, \bar{y}, 1 - z$). The O···O distance is 2.55 Å, and the O—H···O angle is 105°. A second hydrogen bond is possible between O(3) of A and N(1) of B with an O···N distance of 2.93 Å. The lack of hydrogen bonds to ClO_4^- leaves it relatively free, which is reflected in the anisotropic thermal parameters for all oxygen atoms of the ion.

The absorption spectrum of $Ni^{III}L$ in phosphate solutions showed a pH dependence; in acid solutions its color is green whereas above pH 3.8 the solutions turned yellow-orange. The change in color seems to be due to the disappearance of the absorption band at 730 nm (Table I). This pK is attributed to the reaction

$$[Ni^{III}L(H_2PO_4)_2]^+ \rightleftarrows [Ni^{III}L(HPO_4)_2]^- + 2H^+ \qquad p\mathit{K}_a = 3.8 \pm 0.2 \tag{5}$$

An attempt was made to determine the equilibrium constant of the reaction

$$Ni^{III}L^{3+} + 2H_2PO_4^- \rightleftarrows [Ni^{III}L(H_2PO_4)_2]^+ \tag{6}$$

by diluting solutions containing different concentrations of $Ni^{III}L$ and $H_2PO_4^-$ at several pHs and measuring the optical density at 395 nm. The results were complicated and somewhat inconclusive due to the apparent similarity of the absorption spectra of $[Ni^{III}L(H_2PO_4)(H_2O)]^{2+}$, $[Ni^{III}L(H_2PO_4)_2]^+$, $[Ni^{III}L(HPO_4)(H_2O)]^+$, $[Ni^{III}L(HPO_4)_2]^-$, and $Ni^{III}L(HPO_4)(H_2PO_4)$. However the results do indicate $K_{H_2PO_4^-} = [Ni^{III}L(H_2PO_4^-)_2]^+/[NiL^{3+}][H_2PO_4^-]^2 \simeq 2 \times 10^4$ M^{-2} at pH 2.0 in good agreement with the value obtained from the electrochemical results (Table I).

The kinetics of decomposition of $Ni^{III}L$ in phosphate-containing solutions was studied. In all cases the kinetics obeyed a first-order rate law in $Ni^{III}L$. The dependence on phosphate at different pHs and $[Ni^{III}L]$ is plotted in Figure 6. The slopes

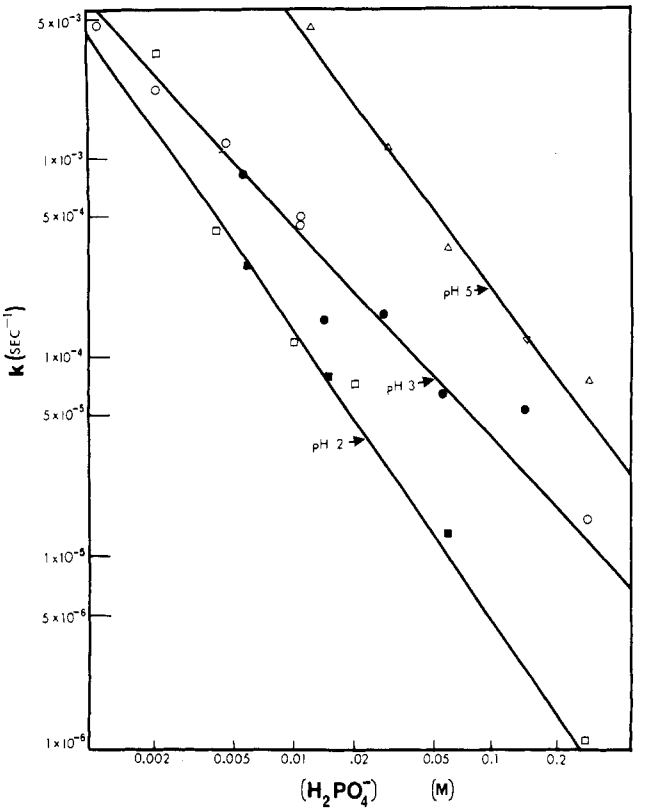

Figure 6. Dependence of the rate of decomposition of $Ni^{III}L$ on $[H_2PO_4^-]$ at different pHs; μ = 0.3 M.

of the lines indicate that the rate of decomposition of $Ni^{III}L$ depends on phosphate concentration according to the equation

$$-\frac{d[N^{III}L]}{dt} = k[Ni^{III}L][H_2PO_4^-]^n$$

where n depends on the pH and $1.1 \leq n \leq 1.5$ in the pH range studied. The observation that $n \geq 1$ indicates that the rate of decomposition of $Ni^{III}L^{3+}$ is larger than that of $[Ni^{III}L(H_2PO_4)(H_2O)]^{2+}$, and that is larger than that of $[Ni^{III}L(H_2PO_4)_2]^+$. The rate of decomposition of the latter complex seems to be neglibile as the half-life of $Ni^{III}L$ in 0.3 M NaH_2PO_4 at pH 2.0 is ca. 5×10^3 longer than that of NiL^{3+}, a result that would give $K_{H_2PO_4^-} \approx 5 \times 10^4$ M^{-2} if one assumes that the only route of decomposition of $Ni^{III}L$ is via NiL^{3+}.

The pH dependence of the rate of decomposition at constant phosphate concentration is plotted in Figure 7. The increase in the rate of decomposition below pH 2.0 seems to be due to the decrease in $[H_2PO_4^-]$. However when the experimental points are corrected for the change in $[H_2PO_4^-]$ with the assumption that the dependence of the rate on the concentration is $[H_2PO_4^-]^{1.5}$, as observed at pH 2.0, the points fall on a straight line. Thus the results indicate a first-order dependence of the rate of decomposition of $Ni^{III}L$ on OH^- in the pH range of 0.7–4.2. Above this pH the rate remains constant for at least 2 pH units. These observations suggest

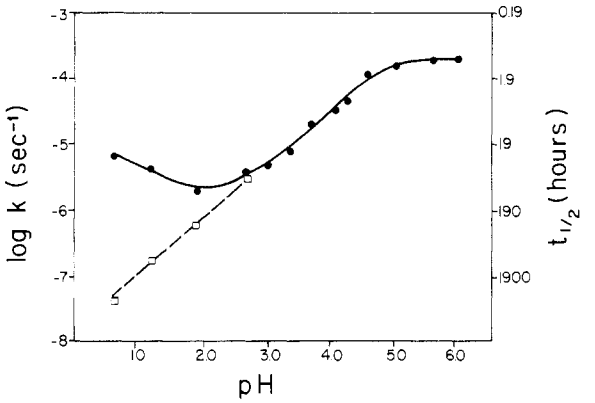

Figure 7. Rate of decomposition of $Ni^{III}L$ as a function of pH in a solution of 0.3 M phosphate at a pH controlled by NaOH, H_3PO_4, or $HClO_4$: (●) experimental points; (□) corrected values to a constant concentration of $H_2PO_4^-$ = 0.3 M for solutions where the pH was controlled by the addition of $HClO_4$, with the assumption of $k_{obsd} \approx [H_2PO_4^-]^{-1.5}$ (see text).

that the increase in concentration of $[Ni^{III}LOH]^{2+}$, $pK_4 = 3.7$, and/or $[Ni^{III}L(HPO_4)_2]^-$, $pK_5 = 3.8$, increases the rate of decomposition of $Ni^{III}L$. As $[Ni^{III}L(H_2PO_4)]^-$ is expected to have properties similar to those of $[Ni^{III}L(SO_4)_2]^-$, the major factor seems to be the increase in $[Ni^{III}LOH]^{2+}$. Above pH 4.2 the concentrations remain nearly constant as this is about 0.5 pH unit above pK_4 and pK_5 and far below the second pK of phosphoric acid.

Concluding Remarks

The results reported in this study indicate that simple anions stabilize NiL^{3+} by axial coordination. The order of the stability constants for axial coordination found ($C_8H_4O_4^{2-} > SO_4^{2-} \geq HPO_4^{2-} > H_2PO_4^- > Cl^- >> ClO_4^-$) is in agreement with the basicity of these ligands.

The absorption spectra of all the complexes studied are similar with the exception of $Ni^{III}LOH^{2+}$, which has a relatively strong absorption band at 550 nm. The latter band was attributed to a distortion of the complex resulting in a pentacoordinated nickel.[7,9] (Further evidence for the pentacoordinated nature of $Ni^{III}LOH^{2+}$ is given in ref 29.) Thus we believe that all the complexes reported in this study are octahedrally coordinated, i.e., $Ni^{III}L(H_2O)_2^{3+}$, $Ni^{III}LX_2$, and $Ni^{III}LXH_2O$.

The results indicate that the mechanism of decomposition of $Ni^{III}LX_2$ is mainly via NiL^{3+} and to some degree via $Ni^{III}LXH_2O$. For X = Cl^- the latter route clearly contributes to the mechanism of decomposition. As the decomposition of the tervalent nickel complexes results in the oxidation of the ligand via introduction of imine groups it was suggested that the first step in the decomposition involves the proton in the

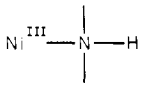

group.[7] Clearly the ligation of anions to the nickel decreases the inductive effect of the nickel on the N–H bond, thus decreasing the acidity of these protons. It is believed that this change in the acidity of the hydrogens bound to the nitrogens is of major importance in the stabilization of the tervalent nickel complex. It should however be noted that axial ligation of sulfate to Ni^{III} cyclam has a considerably smaller stabilizing effect,[30] though the stability constant for ligation is similar to that observed here,[14] an observation indicating that other factors, probably steric ones, affect the rate of decomposition of tervalent nickel complexes with macrocyclic ligands. Studies to clarify this point are in progress.[29]

Acknowledgment. We are indebted to Ms. L. Carmel for technical assistance. A fellowship to E.Z. from the A. K. Casali Foundation is appreciated.

Registry No. $[NiL(H_2PO_4)_2]ClO_4$, 79329-56-9; $[NiL(SO_4)(H_2O)]ClO_4$, 79329-58-1; $NiL(H_2O)_2^{3+}$, 79329-59-2; $NiLCl_2^+$, 79329-60-5; $NiL(SO_4)_2^-$, 79329-61-6; $NiL(C_8H_4O_4)_2^-$, 79329-62-7; $NiL(ClO_4)_2$, 79389-94-9.

Supplementary Material Available: Listings of thermal parameters and observed and calculated structure factors (26 pages). Ordering information is given on any current masthead page.

(29) Zeigerson, E.; Ginzburg, G.; Becker, J. Y.; Kirschenbaum, L. J.; Cohen, H.; Meyerstein, D. *Inorg. Chem.*, in press.
(30) Zeigerson, E.; Ginzburg, G.; Meyerstein, D.; Kirschenbaum, L. J. *J. Chem. Soc., Dalton Trans.* **1980**, 1243.

Contribution from the Chemistry Department, Aligarh Muslim University, Aligarh, U.P., India

Mixed-Ligand Complexes of Trivalent Lanthanide Ions with β-Diketones and Heterocyclic Amines

K. IFTIKHAR, M. SAYEED, and N. AHMAD*

Received November 11, 1980

The diaquo bipyridyl adducts of tris(heptafluorooctanedionato)lanthanide(III), $[Ln(fod)_3bpy\cdot 2H_2O]$, and $[M(fod)_3phen]$ where M = Y, La, or Lu have been synthesized and characterized. The Ln(III) in $[Ln(fod)_3bpy\cdot 2H_2O]$ are 10-coordinate and retain this higher coordination number even in solution for several days without any trace of dissociation. These seem to have achieved their coordinative saturation and therefore $[Pr(fod)_3bpy\cdot 2H_2O]$ does not act as a lanthanide-induced shift reagent. The values of interelectronic and spectral parameters $\bar{\beta}$, $b^{1/2}$, and δ have been computed, and the higher values of δ for the Pr, Nd, and Er complexes indicate higher covalency. Some ligand field parameters ($b^{1/2}$ and T_λ) and oscillator strengths (P) have been calculated, and evidence has been presented to evince the partaking of f orbitals in bonding. The higher values of magnetic moments are also a manifestation of higher coordination number.

Introduction

The paramagnetic tris lanthanide(III) chelates[1] of heptafluoro-7,7-dimethyl-4,6-octanedione (Hfod), $Ln(fod)_3$, have been increasingly used as NMR shift reagents. The chemical property that permits this application is the Lewis acidity that the chelate possesses as a consequence of its coordinative unsaturation. The neutral tris chelates dissolve in organic solvents and form labile adducts with a large variety of nucleophilic substrates. The Lewis acidity of these chelates also causes two side interactions, which may interfere with their usage as NMR shift reagents. Sources of interference are

(1) R. E. Rondequ and R. E. Sievers, *J. Am. Chem. Soc.*, **93**, 1522 (1971); C. C. Hinckley, *ibid.* **91**, 5160 (1969).

0020-1669/82/1321-0080$01.25/0